Polymer 51 (2010) 4037–4043

Contents lists available at ScienceDirect

Polymer

journal homepage: www.elsevier.com/locate/polymer

Functionalization of fluoropolymer surfaces with nanopatterned polyelectrolyte brushes

Sonja Neuhaus [a,b], Celestino Padeste [a,*], Harun H. Solak [a], Nicholas D. Spencer [b]

[a] Laboratory for Micro- and Nanotechnology, Paul Scherrer Institut, 5232 Villigen PSI, Switzerland
[b] Laboratory for Surface Science and Technology, Department of Materials, ETH Zurich, Wolfgang-Pauli-Strasse 10, 8093 Zurich, Switzerland

ARTICLE INFO

Article history:
Received 19 January 2010
Received in revised form
18 May 2010
Accepted 1 July 2010
Available online 23 July 2010

Keywords:
Polyelectrolyte nanostructures
Radiation grafting
EUV interference lithography

ABSTRACT

We present a strategy to combine the excellent bulk properties of fluoropolymer substrates with the wide range of functionalities of surface-grafted polyelectrolyte brushes. Patterns of radicals serving as initiators were created by irradiation with extreme ultraviolet light (EUV) in an interference setup at the Swiss Light Source. From these initiators, brushes of poly(methacrylic acid) or poly(4-vinylpyridine) were grafted in one step by free-radical polymerization. Brushes carrying primary or secondary amines, i.e. poly(vinylamine), poly(allylamine) and poly(*N*-methyl-vinylamine), were obtained by grafting vinylformamide and acrylonitrile followed by hydrolysis or reduction. Periodic patterns with a resolution of 200 nm were achieved, while the thickness of the brushes in unpatterned areas could be controlled over a range of several hundred nanometers by variation of EUV dose and grafting parameters. The maximum dry brush thickness was used to estimate the average molecular weight of the polymer chains.

1. Introduction

Tailoring the surface properties of bulk materials opens a wealth of possibilities, since the crucial interface with the environment or another material can be modified as required. More often than not, a material with bulk properties suitable for a given application does not have the desired surface properties. Fluoropolymers, for instance, exhibit a number of outstanding bulk properties such as high-temperature stability, excellent chemical resistance and low water sorption [1]. However, their hydrophobicity and chemical inertness, although appropriate for many applications, present a considerable challenge for surface modification. The incentive to create functional fluoropolymer surfaces while preserving their excellent bulk properties has led to a number of approaches ranging from surface chemical etching to plasma and irradiation treatments [2,3]. One of the most versatile ways of surface functionalization is the grafting of polymer brushes, as a number of polymerization techniques are applicable and a variety of functional groups can be introduced [4,5]. Polymer brushes consist of arrays of polymer chains with one chain end tethered to the surface. If the chains have a dense lateral packing, i.e. if the distance between the chains is much smaller than the radius of gyration, they are forced to elongate perpendicularly to the surface in a good solvent, resulting in a so-called brush structure. Brushes of polyelectrolytes (PEL) carry charges along the polymer backbone or in the side chains, causing fundamental differences to neutral brushes in terms of chain conformation and response to external parameters. In weak PELs, the charge density can be tuned by changing the pH of the medium, whereas the charges are fixed in strong PELs [6]. As weak PELs respond to simple external parameters, a number of investigations have dealt with the degree of swelling as a function of pH, concentration and nature of the counterions [7–10], as well as pH-induced switching of surface wettability [11]. Typical chemical functionalities in weak PELs include amines and carboxylic acids, which can for instance be used to immobilize molecules on the surface via peptide coupling. Noncovalent immobilization of biomolecules has been reported, whereby their functionality was retained. These promising results could pave the way to polymer-brush-based biosensors [12–15]. PEL brushes are also excellent scaffolds for polyelectrolyte multilayer deposition, as the obtained layer thickness is tunable by varying the conditions during deposition and/or the nature of the underlying brush [16,17]. Polyelectrolytes can be deposited selectively on patterns of charged polymer brushes on a suitable substrate, leading to surface-anchored objects with defined vertical layering. Therefore, the creation of layers of polyelectrolytes on nano-patterned brushes could lead to novel assemblies on the nanoscale.

In this study, radiation-grafting has been used to grow polymers from the surface of fluoropolymers, i.e. poly(ethylene-*alt*-tetrafluoroethylene) (ETFE) foils. Radicals are created directly in the

* Corresponding author. Tel.: +41 563102141.
E-mail address: celestino.padeste@psi.ch (C. Padeste).

0032-3861/$ – see front matter © 2010 Elsevier Ltd. All rights reserved.
doi:10.1016/j.polymer.2010.07.002

polymer substrate by irradiation with electrons or photons, a process established in the production of bulk grafted membranes for fuel cells [18,19]. In order to limit the creation of radicals to the surface, the penetration depth of the radiation must be very small. The "nano-grafting" approach has been developed to fulfill this requirement and to prepare nano-patterned polymer brushes [20,21]. ETFE substrates are exposed to extreme ultraviolet (EUV) light ($E_{ph} = 92$ eV, $\lambda = 13.4$ nm) in an interference setup at the EUV Interference Lithography Beamline (EUV-IL) at the Swiss Light Source (SLS) [22]. The interference of beams diffracted by a silicon nitride (Si_3N_4) membrane mask with chromium gratings creates a pattern of radicals in the topmost 100 nm of the foil (Scheme 1). Upon contact with ambient air, the radicals react to form stable peroxides and hydroperoxides [23,24]. During the grafting procedure, the peroxide moieties are thermally cleaved, yielding radical initiators for free-radical polymerization (FRP).

Here, we present strategies to modify ETFE surfaces with micro- and nanopatterns of weak polyelectrolyte brushes with carboxylic acid or amine functionality. Variation of the exposure dose leads to changes in the grafting density which influences, along with other parameters, the dry brush thickness. The pH of the monomer solution has a large impact on the dry brush thickness in the case of PMAA. Characteristic dependencies of the brush thickness on the exposure dose were observed for different monomers and will be discussed in detail.

2. Experimental section

2.1. Materials

Extruded 100 μm thick films of ETFE (Nowoflon, ET-6235 Nowofol GmBH, Siegsdorf, Germany) were placed between two 4″ silicon wafers and hot pressed for 5 min at 230 °C with an applied pressure of 2 MPa in order to obtain flat surfaces. Acrylonitrile (AN, for synthesis, Merck, Switzerland), *N*-vinylformamide (VF, 98%, Aldrich, Germany), 4-vinylpyridine (4VP, 95%, Aldrich, Germany), borane–THF complex (1 M solution in THF, Aldrich, Germany), NaOH (p.a., Merck, Switzerland), HCl (fuming, 36–38%, Baker, NJ, USA), poly(ethylene glycol) (PEG, average M_n 380-420, Aldrich, Germany) and chloroform (puriss. p.a. ≥ 99.8%, Fluka, Germany) were used as received. Methacrylic acid (MAA, 99%, Aldrich, Germany) was distilled under vacuum prior to use. Water for rinsing or as a solvent was used in Millipore quality.

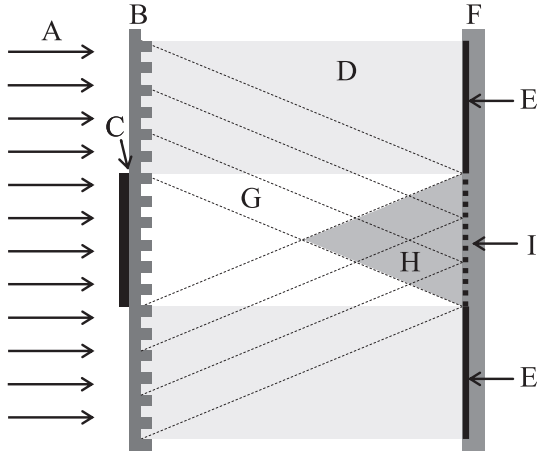

Scheme 1. EUV interference lithography. The incoming beam from the SLS (A) hits a membrane mask (B) with diffraction gratings and a beam stop (C). The direct beam (D) creates an area of high radical density (E = unpatterned region) on the ETFE foil (F), while the 1st order diffracted beams (G, dashed lines) interfere in (H) and create a pattern of radicals (I) on the ETFE surface.

2.2. Exposure

ETFE samples were exposed to extreme ultraviolet (EUV) light at the EUV Interference Lithography Beamline at the Swiss Light Source. Exposures were performed in vacuum ($<5 \times 10^{-6}$ mbar). The beamline uses undulator light with a central wavelength of 13.4 nm (92.5 eV photon energy) and ~3% spectral bandwidth. The incident EUV power on the sample was several mW/cm^2 and the delivered dose was controlled using a fast beam shutter. The samples were irradiated using interfering beams according to the methods described earlier [25]. Patterns of radicals were created on the ETFE surface by irradiation through silicon nitride masks with chromium gratings of different periods. Moreover, areas of higher radical density (without patterning on the nanoscale) were created where the direct, undiffracted beam hit the sample. These areas will subsequently be referred to as "unpatterned". The irradiated samples were stored in a deep freezer at −80 °C.

2.3. Grafting from ETFE surfaces via free-radical polymerization

General procedure: Monomer solutions were degassed with argon for 10 min. The ETFE sample was taken from the deep freezer, rinsed with acetone and dried in a stream of nitrogen. It was then added to the vial containing the monomer solution, which was sealed with a rubber septum and degassed for another 15 min. The vial was placed in an oil bath and heated to the given temperature for the time indicated. After rinsing and washing, the samples were dried with nitrogen.

PMAA: The pH of the methacrylic acid solution (10 vol.-% in H_2O) was adjusted with NaOH or HCl. The polymerization was carried out at 60 °C for 1 h. The grafted sample was rinsed with H_2O. *P4VP*: 4-Vinylpyridine was polymerized from the ETFE surface without added solvent at 60 °C for 1 h. The sample was washed in 0.1 M HCl and immersed therein overnight. *PVF*: The polymerization was carried out in an aqueous solution of *N*-vinylformamide (20 vol.-%) at 70 °C for 2 h. The sample was rinsed with H_2O. *PAN*: the FRP of acrylonitrile (66 vol.-% in PEG) was conducted at 60 °C for 2 h. The sample was washed with water and stored in water overnight.

2.4. Chemical modification on the surface

Hydrolysis of PVF: in order to obtain poly(vinylamine) (PVAm) polymer brushes, the formamide moiety was hydrolyzed in 2 M NaOH at 70 °C for 8 h. The sample was then rinsed with DI water and blown dry with nitrogen. *Reduction of PVF and PAN*: the nitrile or formamide group was reduced in 1 M BH_3 in THF at 50 °C for at least 8 h. The samples were then washed in 0.1 M HCl and immersed therein overnight. Finally, boric acid, a reaction byproduct, was extracted with chloroform at 50 °C for 8 h.

2.5. ATR-IR microscopy

Spectra were recorded on a Hyperion 3000 IR-microscope (Bruker, Switzerland) using an ATR-IR objective with an anvil shaped Ge crystal with 100 μm contact area (Bruker, Switzerland). The ATR crystal contacted the surface with a preset and constant pressure. A Globar source and a KBr beamsplitter were used. Light was collected using dedicated optics and sent to a liquid nitrogen cooled MCT (mercury cadmium telluride) detector of 250 μm × 250 μm size (Infrared Associates, FL, USA). The detector is sensitive between 500 and 10,000 cm^{-1}. Reference spectra were recorded just prior to the actual measurement. Apart from

measurements on the brush covered areas, neighboring substrate areas were also characterized in order to monitor possible substrate damage or modification.

2.6. AFM

Measurements were performed in TappingMode® in air on a Dimension IIIa instrument (Veeco, Germany). Silicon cantilevers with a Si_3N_4 coating and a tip radius of 20 nm, a spring constant of 40 N/m and a resonance frequency of 325 kHz (NSC15/AlBS, Mikromasch, CA, USA, manufacturer's specifications) were used for obtaining images in both height and phase mode. Images were processed with second-order flattening procedures (Nanoscope software, Veeco, Germany). The step-height-measurement function implemented in the program was used to determine the dry thickness of polymer brushes at the edge of unpatterned regions.

2.7. Profilometry

Measurements were performed on a DEKTAK profiler (Veeco, Germany) with a stylus of 2.5 μm radius with an applied load of 5 mg. For each exposure dose, three scans of 250 μm length across unpatterned regions were performed and the obtained thickness values were averaged.

3. Results and discussion

3.1. Strategies for the creation of weak nanopatterned PEL brushes on ETFE

Starting from ETFE substrates carrying peroxide initiators created with EUV-IL, a straightforward approach to obtain weak PEL brushes is via free-radical polymerization (FRP) of charged monomers or monomers with dissociable side groups. A variety of monomers was therefore tested for applicability. The dry thickness of the resulting brushes was measured, which is much lower than the thickness of a polymer brush in the swollen state, i.e. in a good solvent. However, it is more easily and precisely accessible and usually correlates closely with the thickness in the swollen state [26].

The grafting of methacrylic acid (MAA) proceeded smoothly in aqueous solution. The brush thickness (measured in air) could be tuned from less than 100 nm to 700 nm by variation of the exposure dose and the pH of the monomer solution, offering the possibility to grow PMAA brushes of a desired thickness by adjusting simple experimental parameters (Fig. 1).

Thick brushes of P4VP, i.e. a polymer carrying aromatic amines, were also obtained in one step (Scheme 2A), but pH control of the polymerization was not possible due to the insolubility of the monomer in water. The introduction of primary or secondary amines was more problematic, as most monomers with amine functionality suitable for free-radical polymerization are available in the more stable salt form (e.g. 2-aminoethyl methacrylate hydrochloride, AEMA). However, the hydration sphere around highly ionized side groups seems to be incompatible with the hydrophobic ETFE substrate, as grafting of AEMA, diallyldimethyl ammonium chloride and sodium styrene sulfonate from ETFE did not succeed in our experiments. In line with our findings, Shkolnik et al. reported similar observations for the grafting of sulfonated styrene from poly(ethylene) [27]. Neutralization of the side groups is not an option for AEMA, since this monomer undergoes rearrangements at higher pH. Therefore, graft polymerization of a neutral monomer followed by a transformation of the functional groups was applied (Scheme 2B). PEL brushes with primary and secondary amines could be derived from PVF brushes by basic hydrolysis and reduction in borane/THF, respectively. Interestingly,

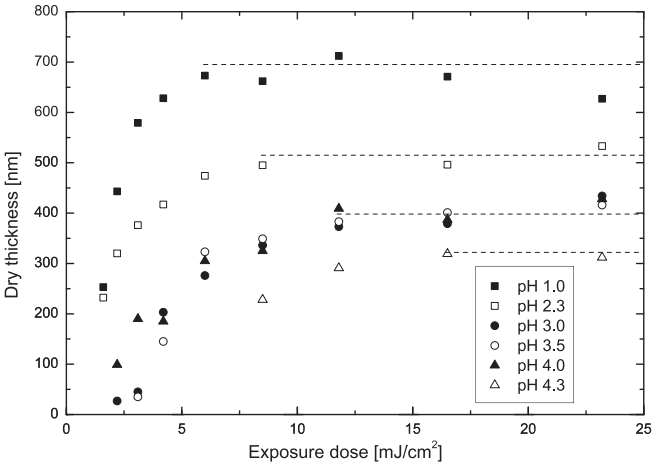

Fig. 1. Dry thickness of PMAA brushes measured with AFM as a function of the exposure dose and the pH of the monomer solution. The maximum thickness is marked for each pH value with a dashed line starting at the dose where saturation was reached. The error in the thickness measurement is estimated to be smaller than 10% of the measured value.

the dependence of the PVF brush thickness on exposure dose was very distinct from that of P4VP brushes (Fig. 2). These findings are detailed in the next section.

PAAm brushes were obtained by grafting of PAN followed by reduction with borane. ATR-IR microscopy of reduced samples showed that boric acid had been incorporated into the substrate and the brush. It could be extracted by washing the samples in chloroform at 50 °C. Other than that, no changes in the substrate were observed after the harsh chemical treatments, confirming the stability of ETFE against the applied conditions. Moreover, the stable

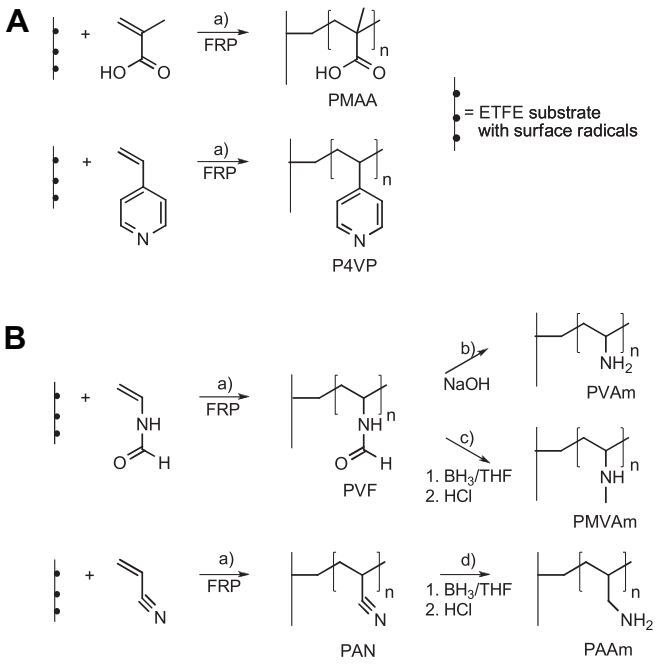

Scheme 2. Strategies for the creation of weak PEL brushes on ETFE substrates: A) FRP of monomers with dissociable side groups; B) graft polymerization of a neutral monomer followed by transformation of functional groups. a) FRP initiated by surface-bound initiators; b) primary amines in PVAm by hydrolysis of PVF in 2 M NaOH; c) secondary amines in PMVAm by reduction of PVF in 1 M borane/THF; d) primary amines in PAAm by reduction of PAN in 1 M borane/THF. Details are given in the experimental section.

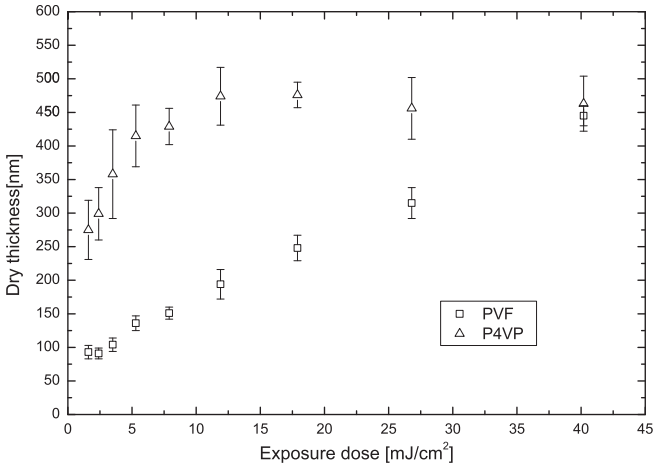

Fig. 2. Dry thickness of PVF and P4VP brushes measured with a profiler as a function of the exposure dose. In the dose range shown, the thickness of PVF brushes increases steadily, while the thickness of P4VP brushes saturates at a low exposure dose.

covalent anchoring of the polymer brushes to the surface also tolerated these treatments.

The presented approaches as summarized in Scheme 2 are very versatile, as a large variety of weak polyelectrolyte brushes can be created. The two-step approach is extendable to strong PEL brushes, e.g. by the sulfonation of poly(styrene) brushes or the quaternization of P4VP brushes. Therefore, the limitations imposed by the incompatibility of certain monomer/substrate combinations or the lack of a suitable monomer can be overcome by the two-step procedure involving grafting and subsequent transformation of functional groups on the surface.

With the strategies presented above, dot patterns with a 283 nm-period, as well as line patterns with a 200 nm-period were routinely obtained (Fig. 3). Note that due to the significantly lower initiator density, the structure thickness in patterned areas is in the tens-of-nanometers rather than in the hundreds-of-nanometers range, as is observed for unpatterned areas. The pattern resolution can be further improved by means of controlled living polymerization methods, such as reversible addition fragmentation transfer (RAFT) [28]. Note that the discussion of the interplay between initiator density and brush thickness in Section 3.3 is based on measurements on unpatterned regions.

3.2. Parameters influencing the polymer dry brush thickness

In one exposure at the EUV-IL beamline, a number of samples can be prepared. On each sample, the exposure dose is varied from one field to another. This allows assessing nine exposure doses in a single free-radical polymerization experiment, ensuring consistent reaction conditions. The exposure dose correlates with the initiator density, and an increase in dry brush thickness with increasing initiator density is naturally observed (Figs. 1 and 2). The grafting conditions such as monomer concentration, solvent and solvent viscosity affect the thickness of the obtained brushes and were adjusted such that the brush regime was reached and the dry thickness was on the same order of magnitude for all monomers. The polymerization times (1–2 h) are long enough to reach the maximum brush thickness obtainable with FRP, as initiator decomposition is fast [29,30] and an almost constant monomer concentration can be expected throughout the polymerization reaction, making the obtained molecular weight dependent on the ratio of the rate constants of propagation and termination, but independent of time [31].

The grafting of P4VP and PVF brushes was well reproducible; the data points shown in Fig. 2 are averages of measurements on several samples. The range over which the brush thickness can be tuned by simply varying the exposure dose is remarkable. The thickness of P4VP brushes saturates at a low exposure dose, while the PVF brush thickness increases steadily in the regime shown, only saturating at a much higher exposure dose. Possible reasons for these trends will be discussed in the next section.

In addition to the exposure-dose dependence discussed above, the thickness of PMAA brushes could be tuned by the pH of the monomer solution as illustrated above (Fig. 1). The thickest brushes were obtained at pH 1, where the MAA monomer is undissociated and neutral. When increasing the pH and therefore the fraction of negatively charged monomers, the brush thickness steadily decreased. Above pH 4.5, MAA could not be grafted from ETFE. For MAA polymerizations in solution, the dependence of the propagation rate on the pH of the monomer solution has been investigated by several groups, resulting in intricate interpretations [32–34]. In our case, two explanations for our observations are possible. Firstly, electrostatic repulsion between growing chain ends and monomer molecules must be considered, as this could hinder the incorporation of more monomers. Secondly, when the degree of dissociation is high, the incompatibility of the negatively charged monomer with the hydrophobic base polymer could hamper polymerization, especially in the initiation step and during the initial brush growth, when the charged monomers are very close to the surface [27]. We assume that a combination of these factors led to the decrease in brush thickness with increasing pH value. The reason notwithstanding, adjusting the pH of the monomer solution offers a straightforward approach to tuning the brush thickness to the desired value over a wide range. The same tunability by pH adjustment was observed in experiments with the grafting of acrylic acid monomers.

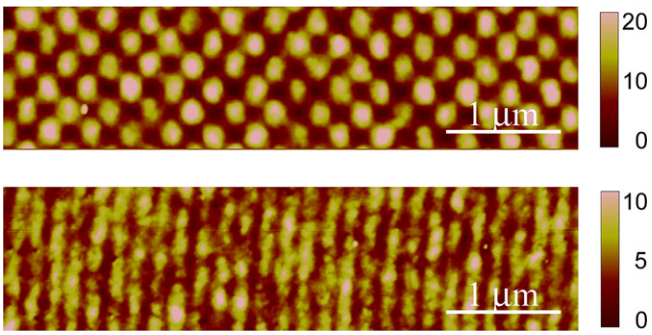

Fig. 3. AFM height images of PMAA structures forming a 283 nm-period dot pattern (top) and a 200 nm-period line pattern. Height scale is in nm.

3.3. Interplay of exposure dose, initiator density and monomer type

The different dependencies of the P4VP, PVF and PMAA brush thickness on exposure dose warrant further consideration. In a former investigation in our group, the diffraction efficiency (f) of a typical Si_3N_4 membrane mask was determined using a CCD camera [28]. In unpatterned areas, roughly 50% of the set dose reached the sample, whereas patterned areas were irradiated with 6–10% of the dose incident on the mask (note that the exposure dose given in the figures always corresponds to the *set* dose). With this information and the photon energy ($E_{ph} = 92$ eV), the number of photons (N_{Ph}) incident on 1 nm^2 at a given exposure dose (D) can be calculated as follows:

$$N_{Ph} = \frac{f \cdot D(\mathrm{J/nm^2})}{E_{Ph}(\mathrm{J})} \quad (1)$$

For example, for a set dose of 10 mJ/cm^2, 3.4 photons would impinge on 1 nm^2 in an unpatterned area and an average of 0.7 photons/nm^2 in a patterned area. Taking the bond energy in the main chain of ETFE as roughly 400 kJ/mol (4 eV/bond), one EUV photon (92 eV) is more than 20 times higher in energy than the bond to be broken [35]. Therefore, we assume that almost every photon incident on the sample is able to create radicals, which are then converted to peroxides or hydroperoxides upon exposure to air [23,24]. These considerations are complicated by radical recombination events and the finite penetration depth of the photons (<100 nm), i.e. some radicals will recombine before they are stabilized and not all of the created radicals will be located near enough to the surface to initiate a chain. However, despite these complications and even if the initiation efficiency was very low, the number of chains grown from the surface should be near to or above the limit for polymer brushes at a moderate exposure dose for high-molecular-weight polymer chains. The dependence of dry thickness (measured on unpatterned areas) on exposure dose observed in Figs. 1 and 2 corroborates this statement. A monotonic increase of dry brush thickness with exposure dose, i.e. with increasing grafting density, is expected in the regime where a decreasing distance between initiating sites forces growing polymer chains to stretch away from the surface. This trend is interrupted, however, when a certain initiator density (corresponding to a certain exposure dose) threshold is crossed. This is the case when there is no space to accommodate additional chains. Therefore, the observed saturation in polymer brush thickness at a given exposure dose implicates a very high grafting density. Following the argument of the geometric constraints on chain initiation and growth, the varying threshold doses for different monomers can be explained. Tsujii and coworkers have introduced the dimensionless grafting density σ^*, which allows comparing different monomers [36]. The cross-sectional area a^2 (i.e. the projection) of a monomer is given by

$$a^2 = \frac{v_0}{l_0} \tag{2}$$

where v_0 is the molecular volume per monomer unit, which is estimated from the bulk density of the monomer, and l_0 is the length of a repeat unit in all-*trans* conformation (0.27 nm). The dimensionless grafting density σ^* is then calculated as

$$\sigma^* = a^2\sigma \tag{3}$$

where σ is the grafting density. A dimensionless grafting density of $\sigma^* = 1$ presents the hypothetical limiting case where the surface is tightly packed with polymer chains in all-*trans* conformation. Very highly stretched PMMA chains, i.e. with a thickness measured in a good solvent approaching 90% of their contour length, were found experimentally for $\sigma^* = 0.4$ by Yamamoto and coworkers [37]. Moreover, the dry thickness of these brushes reached about 40% of the extended chain length, indicating a high degree of stretching even in the dry state. Based on these findings and our experimental evidence pointing to high graft densities in the brush regime, a dimensionless grafting density of $\sigma^* = 0.4$ is assumed in the following. Using eqs. (2) and (3), the cross-sectional area a^2 for the monomers used in this study as well as an estimate for the grafting density σ_{est} was calculated (Table 1).

The results in Table 1 indicate that, the space demand of a 4VP monomer or repeat unit (0.66 nm^2) is 1.5 times larger than for VF repeat units (0.43 nm^2). The fact that a 4VP unit occupies the largest area can be easily appreciated, as it is the only monomer with an aromatic ring, and thus has a stiff and bulky side group. The results presented in Fig. 2 can therefore be explained by the substantially higher space demand of P4VP chains, leading to saturation at low

Table 1
The projected area a^2 of each monomer was calculated from the molecular weight M and the bulk monomer density ρ_m. A dimensionless grafting density of $\sigma^* = 0.4$ was assumed to estimate the grafting density σ_{est}.

Monomer	Molecular weight M (g/mol)	Bulk density ρ_m (g/cm^3)	Area/monomer a^2 (nm^2)	Grafting density σ_{est} (chains/nm^2)
VF	71.08	1.014	0.43	0.9
MAA	86.09	1.015	0.52	0.8
4VP	105.14	0.975	0.66	0.6

exposure doses, while the maximum density of PVF chains is not reached in the dose range shown. On the other hand, it is less clear why the space demand of a PMAA unit should be considerably larger than a PVF unit. A potential explanation is the dimerization of carboxylic acids, which fixes pairs of carboxylic acid side groups in one plane, decreasing the rotational freedom of single bonds and increasing the occupied area. This theory is supported by the ATR-IR spectrum of a PMAA brush grown at low pH (Fig. 4). The C=O band is clearly in the region of hydrogen-bonded carboxylic acids. More evidence for dimerization is the shoulder around 940 cm^{-1}, as this OC–OH deformation (out of plane) band only appears in dimers [38]. Based on this observation, the trend of increasing saturation dose with increasing pH of the monomer solution can also be justified (cf. Fig. 1). With increasing pH, the fraction of charged MAA monomers increases. However, dimerization is not possible for carboxylates, and the fraction of dimers will therefore decrease with increasing pH. As the space demand concomitantly decreases, the saturation dose will be shifted to higher values as clearly observed in Fig. 1.

The estimated grafting density σ_{est} also indicates the approximate number of radicals that need to be created by the EUV photons to obtain saturation. The estimated grafting density is 0.6 chains/nm^2 for P4VP, i.e. a minimum of 0.6 radicals must be created per nm^2. In the case of P4VP, saturation is reached at an exposure dose of about 12 mJ/cm^2, corresponding to 4 photons impinging on 1 nm^2. From these data, the efficiency of the radiation-grafting process, i.e. the number of grafted polymer chains per impinging EUV photon, is estimated to be about 15%. This process leading to a grafted chain is composed of the creation of radicals by EUV photons followed by their stabilization as peroxides, and finally, the initiation and growth of a polymer chain.

As we have measured brush thicknesses in the dry state, the density of the brush ensemble is expected to approach the

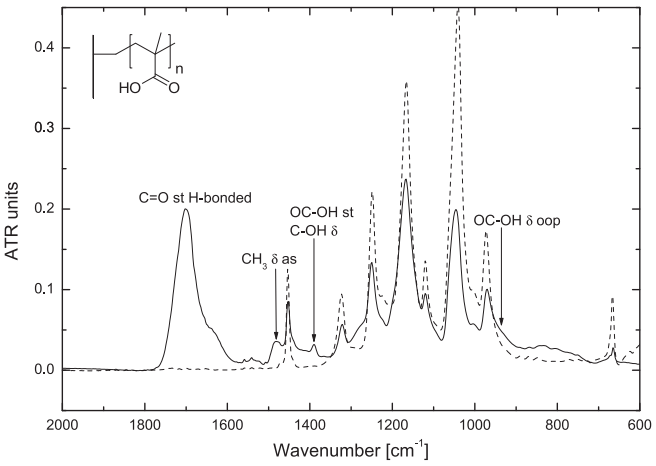

Fig. 4. ATR-IR spectrum of a PMAA brush (solid line) and ETFE (dashed line) for comparison. A number of bands indicate the dimerization of carboxylic acids.

theoretical density of the bulk polymer when saturation is reached. Therefore, the grafting density can be expressed by the following [39]:

$$\sigma = \frac{t\rho_{\mathrm{dry}}N_{\mathrm{A}}}{M_{\mathrm{w}}} \tag{4}$$

where t is the dry brush thickness, M_{w} the molecular weight, ρ_{dry} is the bulk polymer's dry density and N_{A} Avogadro's number. This equation describes the proportionality of the brush thickness to the molecular weight of the polymer chains and the grafting density. Solving the above equation for M_{w} and entering the measured saturation thickness t_{sat} and the estimated grafting density σ_{est},

$$M_{\mathrm{w}} = \frac{t_{\mathrm{sat}}\rho_{\mathrm{dry}}N_{\mathrm{A}}}{\sigma_{\mathrm{est}}} \tag{5}$$

we can roughly estimate the average molecular weight using the values in Table 1 and a typical polymer density of 1.1 g/cm^3. A considerable variation in the grafted polymer chain length is expected due to the free radical character of the polymerization. The results are given in Table 2.

Summing up, the dry brush thickness is a function of the grafting density and the molecular weight of the grafted chains. By varying the exposure dose, the grafting density was experimentally controlled. In the case of MAA, variation of the pH of the monomer solution allowed tailoring of the molecular weight. With this selection of parameters at hand, the thickness of a polymer brush can be adjusted to the desired value.

3.4. Polymer brush integrity and modification of functional groups monitored by ATR-IR microscopy

IR spectroscopy is well suited to confirm the presence of functional groups and their transformation by reduction or hydrolysis. However, the limited area covered by polymer brushes and the fact that the brush is about two orders of magnitude thinner than the ETFE foil necessitates the use of an IR-microscope, which allows for the surface sensitive characterization of defined areas. In the case of P4VP, the pyridine ring skeleton vibrations could be clearly identified (Fig. 5). Features common to all spectra of polymer brushes on ETFE are the bands between 1320 cm^{-1} and 970 cm^{-1}, which are attributed to C–F stretching vibrations and the CH_2 deformation band at 1455 cm^{-1}. The spectra are shown from 2000 cm^{-1} to 600 cm^{-1} because the most important spectral information can be found in this wavenumber range.

The hydrolysis of PVF to PVAm is shown in Fig. 6A. After hydrolysis, the intensities of the amide I and amide II bands were drastically reduced, and the amide NH wagging band disappeared completely. The band at 3265 cm^{-1} associated with the amide NH group was also strongly reduced (cf. Supplementary material). Two NH_2 deformation bands are in evidence in the PVAm spectrum as expected. The hydrolysis of formamide to amine groups was therefore successful, even though it was apparently not quantitative, despite the very long reaction time. It is probable that the thick, dense polymer brushes limited the diffusion of the reactant molecules to functional groups buried at large depth. We can therefore assume that the conversion to amines is higher at the brush surface than at the substrate/brush interface. The reduction of the formamide moiety to yield secondary amines also resulted in

Table 2
Estimation of the average molecular weight of polymer chains in a polymer brush, based on the measured saturation thickness in the dry state t_{sat} and the estimated grafting density σ_{est}.

Polymer	Saturation thickness t_{sat} (nm)	Grafting density σ_{est} (chains/nm^2)	Average molecular weight M_{w} (g/mol)
PVF	1000	0.9	710,000
PMAA	500	0.8	430,000
P4VP	450	0.6	500,000

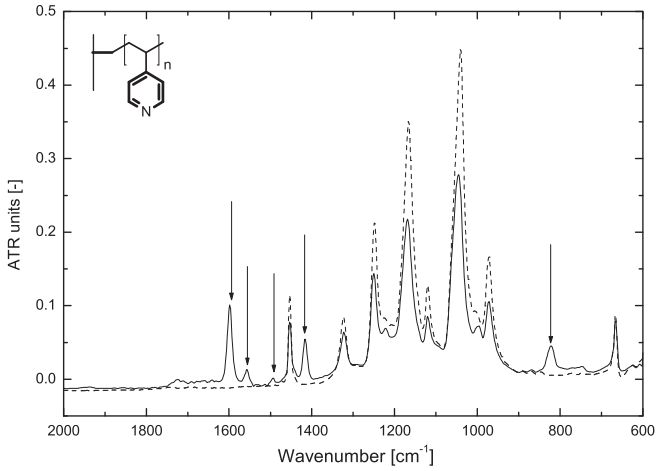

Fig. 5. IR spectrum of a P4VP brush on ETFE recorded on an IR-microscope in ATR mode (solid line). The bands corresponding to pyridine ring skeleton vibrations (marked with arrows) could be clearly identified. The spectrum of the ETFE substrate is shown for comparison (dashed line).

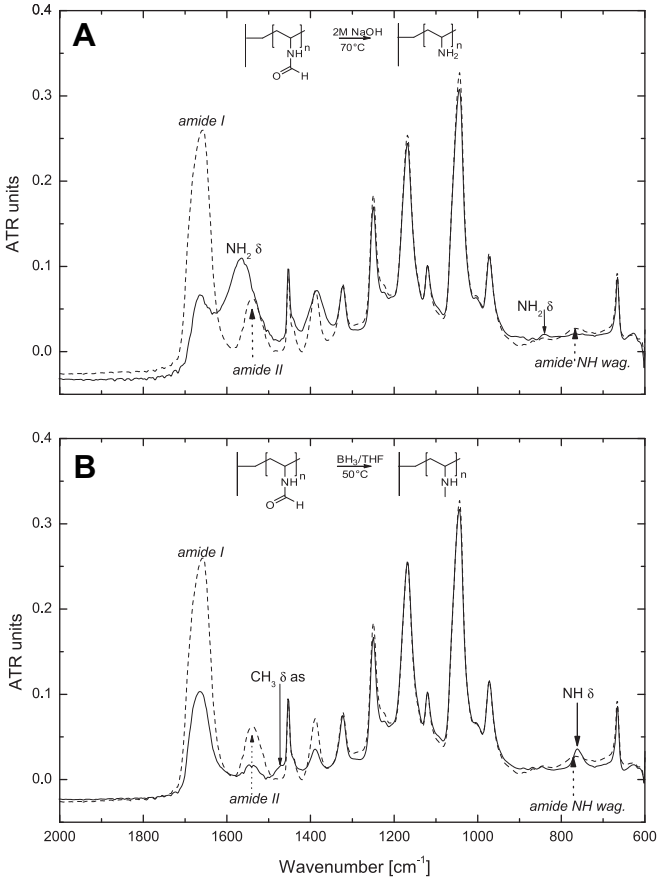

Fig. 6. ATR-IR spectra of PVF as grafted (dashed line) and after hydrolysis (A) and reduction (B) (solid lines). The relevant PVF bands are labeled in italics; the PVAm and PMVAm bands are labeled in normal script.

a drastic decrease in amide band intensity and the spectrum of the resulting PMVAm brush (Fig. 6B) was clearly distinct from that of the PVAm brush. After reduction, the band corresponding to the CH_3 group appeared as a shoulder to the CH_2 deformation band and the amide NH wagging band was replaced by a NH deformation band. The change in intensity in the C–N stretching band (1388 cm^{-1}) hints at a change in the vibrational properties in the two C–N bonds as the side group carbon atom is reduced from –COH to $-CH_3$.

The reduction of the PAN brush resulted in a brush with primary amine functionality, as confirmed by the disappearance of the nitrile peak at 2243 cm^{-1}(cf. Supplementary material). As the PAN brushes had a low dry thickness, the expected weak NH_2 δ band could not be unambiguously identified.

4. Conclusions

We have presented a versatile approach to the modification of fluoropolymer surfaces, which allows the retention and use of their excellent bulk properties. Weak PEL brushes with carboxylic acid and amine functionalities were obtained by the nano-grafting approach and subsequent transformation of functional groups on the surface. Some straightforward experimental parameters influencing the brush thickness were identified and used to tune the latter over a wide range. It was found that the nature and size of the repeat unit strongly influenced the exposure dose required to reach saturation. Average molecular weights in the range of 400,000–700,000 g/mol were reached in the free-radical graft polymerization as estimated from the dry thickness of the brushes at saturation. Furthermore, the efficiency with which an impinging EUV photon finally leads to a grafted polymer chain could be estimated to reach ~15%.

Acknowledgement

The authors thank Konrad Vogelsang and Drs. Hans-Christian Sigg, Philippe Lerch and Luca Quaroni for their assistance. EUV interference lithography exposures were performed at the Swiss Light Source, Paul Scherrer Institut, Villigen, Switzerland. The financial support of the Swiss National Science Foundation (SNF) is greatly appreciated.

Appendix. Supplementary material

Supplementary data associated with this article can be found, in the online version, at doi:10.1016/j.polymer.2010.07.002.

References

[1] Scheirs J. Modern fluoropolymers: high performance polymers for diverse applications. 1st ed. Chichester, UK: Wiley; 1997.
[2] Garbassi F, Morra M, Occhiello E. Polymer surfaces – from physics to technology. Chichester, UK: John Wiley & Sons Ltd; 1998.
[3] Kang ET, Zhang Y. Advanced Materials 2000;12(20):1481–94.
[4] Edmondson S, Osborne VL, Huck WTS. Chemical Society Reviews 2004;33 (1):14–22.
[5] Kato K, Uchida E, Kang ET, Uyama Y, Ikada Y. Progress in Polymer Science 2003;28(2):209–59.
[6] Ruhe J, Ballauff M, Biesalski M, Dziezok P, Grohn F, Johannsmann D, et al. Polyelectrolyte brushes. In: Jordan R, editor. Advances in Polymer Science, vol. 165. Heidelberg: Springer Verlag; 2004. p. 79–150.
[7] An SW, Thirtle PN, Thomas RK, Baines FL, Billingham NC, Armes SP, et al. Macromolecules 1999;32(8):2731–8.
[8] Biesalski M, Ruhe J. Macromolecules 2002;35(2):499–507.
[9] Konradi R, Ruhe J. Macromolecules 2005;38:4345–54.
[10] Zhou JH, Wang G, Hu JQ, Lu XB, Li JH. Chemical Communications 2006; (46):4820–2.
[11] Zhou F, Huck WTS. Chemical Communications 2005;(48):5999–6001.
[12] Kurosawa S, Aizawa H, Talib ZA, Atthoff B, Hilborn J. Biosensors & Bioelectronics 2004;20(6):1165–76.
[13] Rosenfeldt S, Wittemann A, Ballauff M, Breininger E, Bolze J, Dingenouts N. Physical Review E 2004;70(6).
[14] Hollmann O, Gutberlet T, Czeslik C. Langmuir 2007;23(3):1347–53.
[15] Senaratne W, Andruzzi L, Ober CK. Biomacromolecules 2005;6(5):2427–48.
[16] Zhang HN, Ruhe J. Macromolecules 2003;36(17):6593–8.
[17] Zhang HN, Ruhe J. Macromolecules 2005;38(26):10743–9.
[18] Gubler L, Prost N, Gursel SA, Scherer GG. Solid State Ionics 2005;176 (39–40):2849–60.
[19] Gubler L, Gursel SA, Scherer GG. Fuel Cells 2005;5(3):317–35.
[20] Brack HP, Padeste C, Slaski M, Gursel SA, Solak HH. Journal of the American Chemical Society 2004;126(4):1004–5.
[21] Padeste C, Solak HH, Brack HP, Slaski M, Gursel SA, Scherer GG. Journal of Vacuum Science & Technology B 2004;22(6):3191–5.
[22] Auzelyte V, Dais C, Farquet P, Grutzmacher D, Heyderman LJ, Luo F, et al. Journal of Micro-Nanolithography Mems and Moems 2009;8(2).
[23] Suzuki M, Kishida A, Iwata H, Ikada Y. Macromolecules 1986;19(7):1804–8.
[24] Suzuki M, Yamada Y, Iwata H, Ikada Y. Physicochemical aspects of polymer surfaces. New York: Plenum Press; 1983.
[25] Solak HH, David C, Gobrecht J, Golovkina V, Cerrina F, Kim SO, et al. Microelectronic Engineering 2003;67–8:56–62.
[26] Wu T, Efimenko K, Vlcek P, Subr V, Genzer J. Macromolecules 2003;36 (7):2448–53.
[27] Shkolnik S, Behar D. Journal of Applied Polymer Science 1982;27(6):2189–96.
[28] Farquet P, Padeste C, Solak HH, Gursel SA, Scherer GG, Wokaun A. Macromolecules 2008;41(17):6309–16.
[29] Farquet P, Kunze A, Padeste C, Solak HH, Guersel SA, Scherer GG, et al. Polymer 2007;48(17):4936–42.
[30] Kulik EA, Ivanchenko MI, Kato K, Sano S, Ikada Y. Journal of Polymer Science Part a-Polymer Chemistry 1995;33(2):323–30.
[31] Elias H-G. Macromolecules – chemical structure and synthesis. Weinheim: Wiley-VCH Verlag GmbH&Co. KGaA; 2005.
[32] Lacik I, Ucnova L, Kukuckova S, Buback M, Hesse P, Beuermann S. Macromolecules 2009;42(20):7753–61.
[33] Kabanov VA, Topchiev DA, Karaputa TM. Journal of Polymer Science Part C-Polymer Symposium 1973;(42):173–83.
[34] Katchalsky A, Blauer G. Transactions of the Faraday Society 1951;47 (12):1360–70.
[35] Luo Y-R. Handbook of bond dissociation energies in organic compounds. Boca Raton, FL: CRC Press; 2003.
[36] Tsujii Y, Ohno K, Yamamoto S, Goto A, Fukuda T. Structure and properties of high-density polymer brushes prepared by surface-initiated living radical polymerization. In: Jordan R, editor. Advances in Polymer Science, vol. 197. Heidelberg: Springer-Verlag; 2006. p. 1–45.
[37] Yamamoto S, Ejaz M, Tsujii Y, Fukuda T. Macromolecules 2000;33(15): 5608–12.
[38] Pretsch E, Bühlmann P, Badertscher M. Structure determination of organic compounds. 4th ed. Berlin: Springer; 2009.
[39] Sofia SJ, Premnath V, Merrill EW. Macromolecules 1998;31(15):5059–70.